Increasing intracellular magnesium levels with the 31-amino acid MgtS protein

Hanbo Wang[a,b,1], Xuefeng Yin[a,c,1,2], Mona Wu Orr[a], Michael Dambach[a,3], Rebecca Curtis[a,4], and Gisela Storz[a,5]

[a]Division of Molecular and Cellular Biology, Eunice Kennedy Shriver National Institute of Child Health and Human Development, Bethesda, MD 20892-5430; [b]School of Biomedical Sciences, Faculty of Medicine, Chinese University of Hong Kong, Shatin, New Territories, Hong Kong; and [c]Health Science Center, Peking University, Beijing 100191, China

Contributed by Gisela Storz, April 18, 2017 (sent for review February 28, 2017; reviewed by Mark Goulian and Michael T. Laub)

Synthesis of the 31-amino acid, inner membrane protein MgtS (formerly denoted YneM) is induced by very low Mg^{2+} in a PhoPQ-dependent manner in *Escherichia coli*. Here we report that MgtS acts to increase intracellular Mg^{2+} levels and maintain cell integrity upon Mg^{2+} depletion. Upon development of a functional tagged derivative of MgtS, we found that MgtS interacts with MgtA to increase the levels of this P-type ATPase Mg^{2+} transporter under Mg^{2+}-limiting conditions. Correspondingly, the effects of MgtS upon Mg^{2+} limitation are lost in a Δ*mgtA* mutant, and MgtA overexpression can suppress the Δ*mgtS* phenotype. MgtS stabilization of MgtA provides an additional layer of regulation of this tightly controlled Mg^{2+} transporter and adds to the list of small proteins that regulate inner membrane transporters.

PhoP | MgtA | FtsH | small protein | transporters

Bacteria live in rapidly changing environments, most of which are suboptimal for growth, and use a variety of signal transduction mechanisms to promptly respond to these varied conditions. The response mechanisms include an extensive array of two-component signal transduction systems, which typically consist of a membrane-associated sensor kinase and its cognate response regulator, usually a transcription factor (reviewed in ref. 1). One two-component system, PhoPQ, has been shown to be critical to the virulence of many Gram-negative bacteria, including uropathogenic *Escherichia coli* and *Salmonella enterica*, where the system is best characterized (reviewed in ref. 2). When *S. enterica* cells encounter a variety of stress conditions, including low Mg^{2+} levels, an acidic environment, and/or presence of antimicrobial peptides, some conditions that are present in host phagocytes, the sensor kinase PhoQ is activated, leading to the phosphorylation of the response regulator PhoP (reviewed in ref. 3). Activated PhoP in turn induces transcription of a large regulon and thereby promotes Mg^{2+} import, lipopolysaccharide (LPS) modification, and increased resistance to acid and antimicrobial peptides (reviewed in ref. 4), thus promoting survival.

In response to environmental signals, bacteria also induce the synthesis of small regulatory RNAs (sRNAs) and, as has been found more recently, small proteins that also act as regulators. Genes encoding small proteins of 50 amino acids or fewer in length are inadequately annotated in all organisms (reviewed in ref. 5). The *E. coli* chromosome encodes more than 60 confirmed small protein-encoding genes (6), but the physiological roles of the majority are unknown. However, many are conserved and/or are synthesized under very specific environmental conditions (6, 7), implying that they perform critical functions. More than half of the small proteins are predicted to contain an α-helical transmembrane (TM) domain (6), indicating membrane association.

Several small transmembrane proteins have been found to be expressed upon Mg^{2+} limitation and/or have roles in Mg^{2+} homeostasis. For instance, the 47-aa *E. coli* PhoQP-induced MgrB protein interacts with the sensor kinase PhoQ and represses the autophosphorylation of the kinase, thus forming a negative feedback loop that controls the dynamics of PhoP-target gene expression (8, 9). MgrB carries three cysteines and also modulates PhoQ activity in response to changes in the oxidizing environment of the periplasm in *E. coli* and *S. enterica* (10, 11). The 30-aa *S. enterica* MgtR protein is coexpressed with its interaction partner MgtC from PhoPQ-regulated *mgtCBR* operon (12). MgtR mediates the FtsH-dependent degradation of MgtC (12), a membrane-bound repressor of the F_0α-subunit of the F_1F_0 ATP synthase (13). MgtR also interacts with MgtA, a P-type ATPase Mg^{2+} importer to promote turnover, possibly as a mechanism to balance the levels of the MgtA and MgtB transporters under conditions of low Mg^{2+} (14). These examples support the general model that small membrane proteins are induced under specific conditions to interact with and modulate the functions of large membrane proteins.

The 31-amino acid YneM protein, here renamed MgtS, was first predicted as a conserved small ORF in various enterobacterial species (15) in the intergenic region between *ydeE*, encoding a predicted transporter, and *ydeH* (now *dgcZ*), encoding a diguanylate cyclase (Fig. 1*A*). Subsequent studies confirmed that this small protein is synthesized in *E. coli* (6). MgtS is predicted to contain a single hydrophobic α-helix, and assays of alkaline phosphatase and green fluorescent protein fusions to MgtS showed that the 31-amino acid protein spans the inner membrane and adopts a C_{in}–N_{out} orientation (16). It was also discovered that a small, regulatory RNA named MgrR is expressed convergently from *mgtS* in the *ydeE–dgcZ* intergenic region and that transcription of both the MgrR sRNA and the *mgtS* (*yneM*) mRNA is induced by low Mg^{2+} in a PhoPQ-dependent manner (17). Here we report that MgtS acts to increase the intracellular Mg^{2+} concentration thus enabling growth under Mg^{2+}-limiting conditions by increasing the levels of the Mg^{2+} transporter MgtA.

Significance

Proteins of fewer than 50 amino acids are overlooked by most genomic and biochemical approaches and their functions are generally unknown. Here we report that a 31-amino acid inner membrane protein synthesized in response to limiting Mg^{2+} binds and stabilizes the major Mg^{2+} importer, thereby leading to increased intracellular levels of this critical ion. This discovery further supports the hypothesis that many of these overlooked small proteins regulate the functions and stabilities of larger membrane proteins.

Author contributions: H.W., X.Y., M.W.O., M.D., and G.S. designed research; H.W., X.Y., M.W.O., M.D., and R.C. performed research; H.W., X.Y., M.W.O., M.D., R.C., and G.S. analyzed data; and H.W., X.Y., M.W.O., M.D., and G.S. wrote the paper.

Reviewers: M.G., University of Pennsylvania; and M.T.L., Massachusetts Institute of Technology.

The authors declare no conflict of interest.

[1]H.W. and X.Y. contributed equally to this work.

[2]Present address: The Boston Consulting Group, New York, NY 10001.

[3]Present address: NASA Research and Education Support Services, Arlington, VA 22202.

[4]Present address: Fluor, Sugar Land, TX 77478.

[5]To whom correspondence should be addressed. Email: storzg@mail.nih.gov.

This article contains supporting information online at www.pnas.org/lookup/suppl/doi:10.1073/pnas.1703415114/-/DCSupplemental.

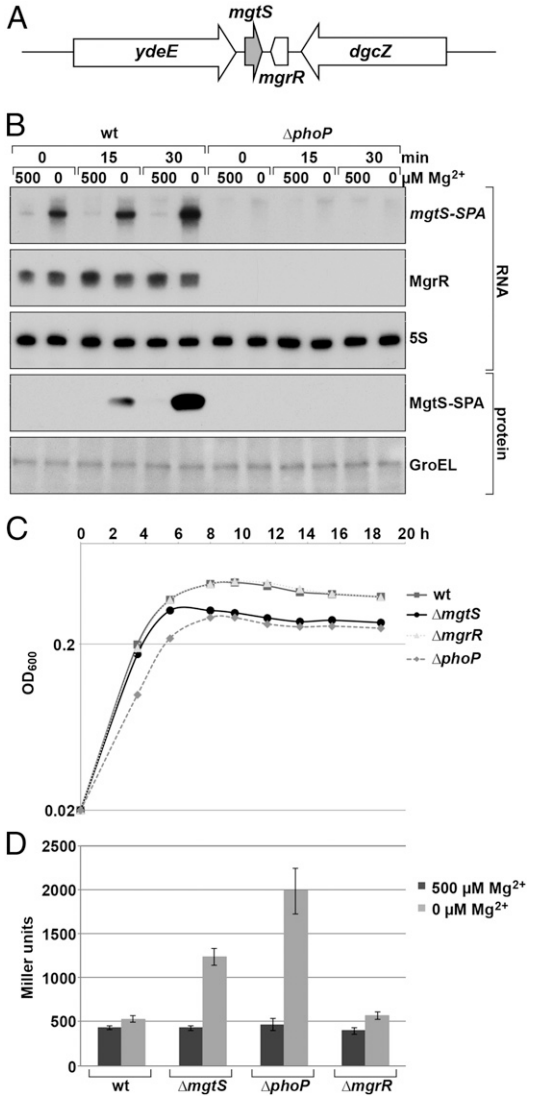

Fig. 1. MgtS contributes to cell growth and intracellular Mg^{2+} upon Mg^{2+} limitation. (*A*) The *mgtS* gene is located between *ydeE* and *mgrR*, encoding a PhoPQ-regulated sRNA. *mgtS* and *mgrR* do not overlap. (*B*) Expression of MgtS-SPA is induced by Mg^{2+} starvation in a PhoP-dependent manner. Northern and immunoblot analyses were carried out for *mgtS-SPA phoP*$^+$ (GSO767) and *mgtS-SPA* Δ*phoP::kan* (GSO768) strains grown in N medium with 500 μM Mg^{2+} or without added Mg^{2+} as described in *SI Appendix*. (*C*) Δ*mgtS* strain shows survival defect upon Mg^{2+} limitation. The OD_{600} of the cultures of wild-type (MG1655), Δ*mgtS::kan* (GSO229), Δ*mgrR::kan* (GSO769), and Δ*phoP::kan* (GSO766) cells grown in N medium containing 7.5 μM Mg^{2+} was measured at the indicated times. The average of three cultures is shown. (*D*) Cells lacking MgtS exhibit elevated Mg^{2+}-reporter activity upon Mg^{2+} limitation. β-Galactosidase activity was assayed for cultures of wild-type (GSO770), Δ*mgtS::kan* (GSO772), Δ*mgrR::kan* (GSO773), and Δ*phoP::kan* (GSO771) cells carrying the chromosomal P_{lac}-5′-UTR_{mgtA}-*lacZ* fusion grown in N medium with 500 μM Mg^{2+} or without added Mg^{2+} as described in *SI Appendix*. The average of three independent assays is shown (error bars represent one SD).

Results

Synthesis of the 31-Amino Acid Membrane Protein MgtS Is Induced by Low Mg^{2+}. To examine the kinetics of MgtS induction upon Mg^{2+} limitation, we assayed the levels of a derivative with a sequential peptide affinity (SPA)-tag (18) expressed from the endogenous chromosomal locus (MgtS-SPA). We first compared the levels of the *mgtS-SPA* mRNA from cells grown in N-minimal medium supplemented with 500 μM $MgSO_4$ or without added Mg^{2+}. Little *mgtS-SPA* mRNA could be detected from bacteria grown with 500 μM Mg^{2+} (Fig. 1*B*). In contrast, *mgtS-SPA* mRNA was seen immediately postwashing with N medium without added Mg^{2+} and continued to increase upon growth. This induction by Mg^{2+} depletion was dependent on PhoPQ as it was completely abolished in a Δ*phoP* strain. We also probed the same blot for the known PhoPQ-regulated MgrR sRNA. In the wild-type but not Δ*phoP* strain, MgrR was detected upon growth in N medium with both 500 and 0 μM Mg^{2+}, in agreement with previous observations that the *mgrR* promoter is induced by a broader range of low Mg^{2+} concentrations (17). We next assayed the MgtS-SPA protein levels. Consistent with the Northern results, MgtS-SPA protein was not detected during growth in medium with 500 μM Mg^{2+}, whereas levels were partially induced by 15 min and dramatically elevated by 30 min after transition into N medium without added Mg^{2+} (Fig. 1*B*).

MgtS Protects Cells at Low Intracellular Mg^{2+} Levels. Given the strong induction of MgtS-SPA by very low Mg^{2+}, we examined the consequences of deleting *mgtS* under conditions of Mg^{2+} limitation. When wild-type cells were inoculated into N medium with a sparing amount of Mg^{2+} (7.5 μM), cultures grew for ∼6 h, after which the OD_{600} plateaued, presumably due to Mg^{2+} exhaustion (Fig. 1*C* and *SI Appendix*, Fig. S1). Δ*phoP* cells had a reduced doubling time initially and could not reach the same OD_{600} as wild-type cells (Fig. 1*C*). Cells lacking MgtS had the same initial doubling time as wild-type cells until 6 h postmedia switch, but also reached a lower final OD_{600} with fewer colony forming units (Fig. 1*C* and *SI Appendix*, Fig. S1). In contrast, the mutant lacking the convergently transcribed sRNA MgrR had a growth curve like the wild-type strain. Because the lower OD_{600} observed for the Δ*mgtS* strain could be complemented by expressing *mgtS* on a plasmid (see *Effect of MgtS Is Reduced in an* mgtA *Deletion Background*), these observations suggest that MgtS is important for cell growth and/or viability when Mg^{2+} is exhausted.

The Mg^{2+}-specific defect of the Δ*mgtS* mutant could be due to a decrease in the intracellular level of Mg^{2+} and/or an inability of the cells to use Mg^{2+}. To evaluate the cause of the defect, we created a reporter for intracellular Mg^{2+} levels by fusing *lacZ* to the Mg^{2+}-responsive 5′-untranslated region (UTR) of *E. coli mgtA*. Depending on the intracellular Mg^{2+} concentration, the *mgtA* 5′-UTR has been shown to adopt alternative RNA secondary structures, which modulates transcription elongation into the *mgtA* ORF through sequestration of a Rho-dependent transcription terminator (19–21). Specifically, elongation into *mgtA* is increased when free intracellular Mg^{2+} levels are low, whereas the transcript is terminated in the 5′-UTR when Mg^{2+} levels are high. Transcription of the *lacZ* reporter remained low in all strains grown in 500 μM Mg^{2+}, indicating higher levels of intracellular Mg^{2+} (Fig. 1*D*). In the wild-type and Δ*mgrR* backgrounds, the P_{lac}-5′-UTR_{mgtA}-*lacZ* fusion is induced minimally 30 min after cells are transferred to N medium without added Mg^{2+} (Fig. 1*D*). In contrast, the fusion is induced 2.9-fold in the Δ*mgtS* mutant and 4.3-fold in the Δ*phoP* mutant. This induction indicates that, upon Mg^{2+} depletion, Δ*mgtS* cells, like Δ*phoP* cells, have lower intracellular Mg^{2+} levels than wild-type cells.

MgtA Copurifies with Functional Tagged Derivatives of MgtS. To learn more about how MgtS acts to affect intracellular Mg^{2+} levels, we sought to identify proteins associated with MgtS. Because we needed negative control mutants and an active-tagged form of the protein, we set out to determine which of the 31 amino acids are important for MgtS activity (Fig. 2*A*). We mutated six highly conserved residues to alanine and assayed the effects of overexpressing the mutants on expression of the P_{lac}-5′-UTR_{mgtA}-*lacZ* reporter in a Δ*mgtS* background (Fig. 2*B*). With the empty vector, reporter expression was elevated 2.0-fold upon growth in N medium without added Mg^{2+} compared with media with 500 μM Mg^{2+}. Overexpression of the wild-type MgtS eliminated induction of the reporter. The G19A, L21A, and S26A mutants had wild-type activity and the W29A mutant had an intermediate phenotype,

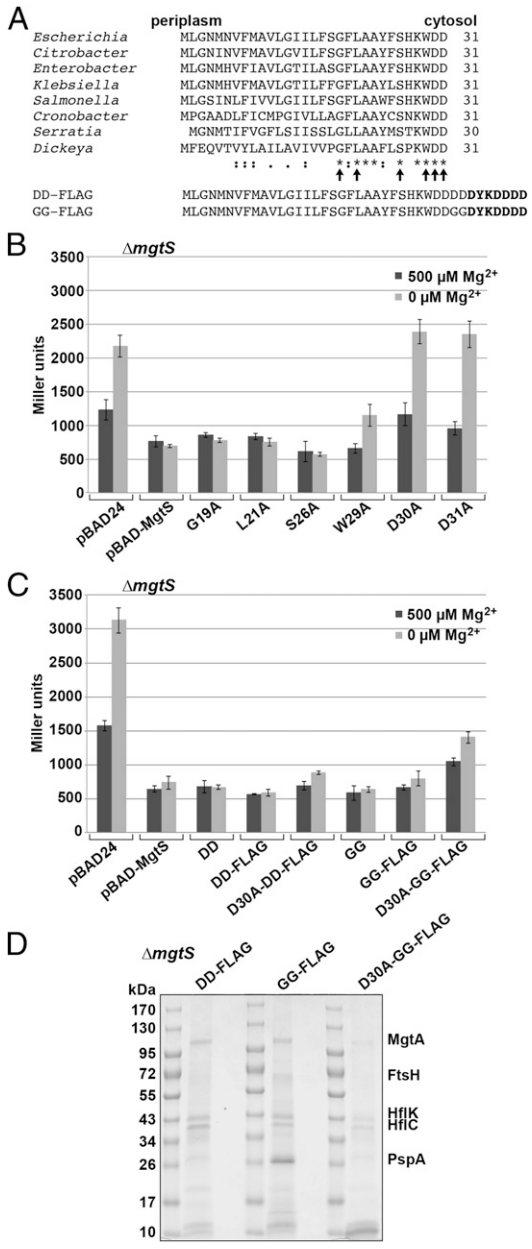

Fig. 2. MgtA Mg^{2+} transporter copurifies with MgtS. (*A*) MgtS is present in multiple enterobacteriaceae species. The sequences shown were aligned using ClustalW (www.ebi.ac.uk/Tools/msa/clustalw2/). MgtS contains one predicted TM domain with the C terminus in the cytoplasm (16). The arrows indicate the alanine-substitution mutants generated. The sequences of the DD-FLAG and GG-FLAG derivatives are shown below the alignment, with the modified FLAG tag indicated in bold. (*B*) D30A and D31A derivatives of MgtS are defective. (*C*) DD-FLAG and GG-FLAG derivatives of MgtS are active. For both *B* and *C*, β-galactosidase activity was assayed for cultures of P_{lac}-5′-UTR$_{mgtA}$-*lacZ* Δ*mgtS* (GSO774) cells carrying pBAD24 expressing indicated derivatives of MgtS as described in *SI Appendix*. The average of two independent trials is shown (error bars represent one SD). (*D*) MgtA copurifies with tagged MgtS. Cultures of Δ*mgtS* (GSO775) cells carrying pBAD24 expressing indicated derivatives of MgtS were grown in N medium with 15 μM Mg^{2+}. Lysates were prepared and mixed with M2 anti-FLAG antibodies conjugated to Sepharose beads as described in *SI Appendix*. Bound proteins were analyzed by SDS/PAGE, and prominent bands were identified as MgtA, HflK, HflC, and PspA by mass spectrometry.

whereas the D30A and D31A mutants had the same activity as the empty vector, indicating the latter two mutants are nonfunctional. We also determined the activity of MgtS mutants expressed from the chromosome. The results of growth upon Mg^{2+} depletion correlated with the effects on 5′-UTR$_{mgtA}$-*lacZ* reporter activity; G19A and L21A grew similarly to the wild-type strain, whereas D30A and D31A grew like the Δ*mgtS* strain, and W29A was intermediate between wild-type strain and deletion mutant (*SI Appendix*, Fig. S2*A*). The exception was S26A, which was only partially functional in the growth assay. Immunoblot analysis of the D30A mutant derivative fused to a FLAG tag indicates the mutant was expressed at wild-type levels or higher, indicating decreased protein levels do not account for the loss-of-function phenotype (see Fig. 3).

Next, we found that neither the C-terminally SPA-tagged nor a C-terminally His_6-tagged wild-type version of MgtS could rescue growth of the Δ*mgtS* strain in low Mg^{2+} (*SI Appendix*, Fig. S2*B*). To determine whether any residues could be added to the C terminus without compromising function, we constructed derivatives containing two additional aspartate residues (D32 and D33) or two glycine residues (G32 and G33). Both extended mutants were functional (*SI Appendix*, Fig. S2*B*). We thus used these two amino acid extensions as linkers for a short epitope consisting of a modified FLAG tag (DYKDDDD, referred to as FLAG throughout) (Fig. 2*A*). Both linker FLAG-tagged derivatives of MgtS were functional in the 5′-UTR$_{mgtA}$-*lacZ* reporter assay (Fig. 2*C*). We noted that the D30A derivative of the DD-FLAG–tagged protein also was almost fully functional when overexpressed, possibly due to the extra aspartate residues in the linker compensating for the reduced charge. However, the MgtS-D30A-GG-FLAG mutant was only partially functional and thus was selected for use as a negative control.

To identify proteins associated with MgtS, cells were grown in 15 μM Mg^{2+} to exponential phase, and MgtS-DD-FLAG, MgtS-GG-FLAG, or the MgtS-D30A-GG-FLAG control were overexpressed from pBAD24. Extracts from each culture were applied to M2 anti–FLAG-affinity columns in the presence of 500 μM Mg^{2+}, and the eluates from each of the columns were analyzed by SDS/PAGE (Fig. 2*D*). The proteins present in the most prominent bands were identified by mass spectrometry. A band identified as the P-type ATPase Mg^{2+} transporter MgtA was specifically enriched in the DD-FLAG and GG-FLAG samples compared with the D30A-GG-FLAG sample. A faint band identified as the membrane protease FtsH was also more prominent for the wild-type constructs, whereas bands corresponding to the HflK and HflC proteins, which form a complex with FtsH, were detected for all of the samples. Finally, a strong band corresponding to the phage shock protein PspA was only prominent for the GG-FLAG sample. The finding that MgtA specifically copurifies with the active forms of MgtS was of interest, given the Δ*mgtS* phenotypes (Fig. 1 *C* and *D*) upon Mg^{2+} limitation.

MgtS Copurifies with MgtA. To test the association between MgtS and MgtA, we carried out reciprocal copurifications using C-terminally tagged derivatives of MgtA shown to be functional in vitro (22). In a first experiment, cells expressing either MgtA-His_6 or a control inner membrane protein AcrB-His_6 were mixed with cells expressing either MgtS-GG-FLAG or MgtS-D30A-GG-FLAG. The mixed cells, as well as unmixed control samples, were homogenized and incubated with the mild detergent dodecyl β-D-maltoside (DDM) to facilitate mixing of the membrane fractions. All samples were then applied to nickel-nitrilotriacetic acid (Ni-NTA) resin. After washing, the proteins retained on the beads were examined by immunoblot analysis with either anti-His or anti-FLAG antibodies (Fig. 3*A*). Both MgtA-His_6 and AcrB-His_6 were detected in the eluates of the unmixed cells as well as in the cells mixed with MgtS-GG-FLAG and MgtS-D30A-GG-FLAG cells, consistent with retention of both His_6-tagged proteins on the Ni-NTA resin. The FLAG-tagged MgtS derivatives were not detected in the eluates of the unmixed cells. In contrast, a strong signal was observed for MgtS-GG-FLAG cells mixed with the MgtA-His_6 but not the AcrB-His_6 cells. These results support the conclusion that the functional MgtS-GG-FLAG fusion protein associates with MgtA-His_6. A significantly weaker signal was detected

MICROBIOLOGY

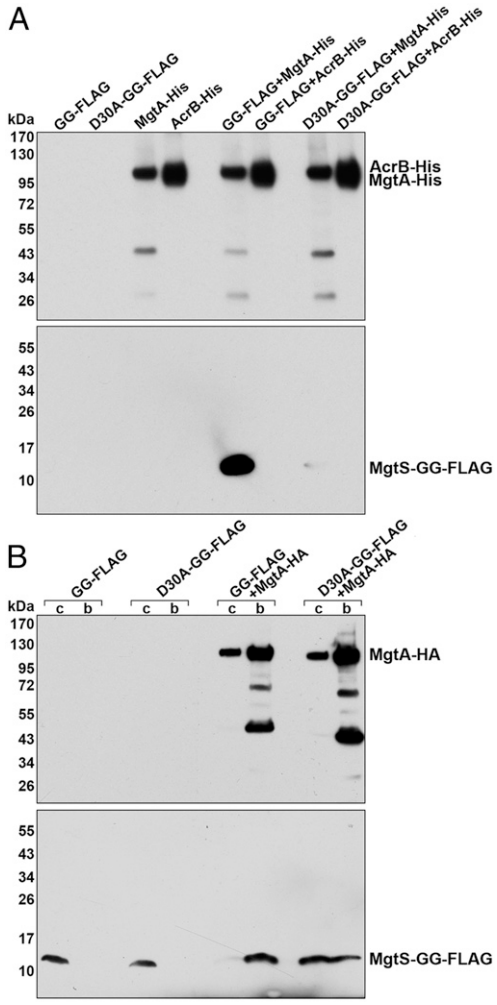

Fig. 3. MgtS copurifies with MgtA. (*A*) MgtS-GG-FLAG copurifies with MgtA-His_6 in cell extracts. Δ*mgtS* mutant cells (GSO776) carrying pBAD24 derivatives expressing MgtS-GG-FLAG or MgtS-D30A-GG-FLAG were mixed with Δ*mgtS* mutant cells (GSO775) carrying pBAD24 derivatives expressing MgtA-His_6 or AcrB-His_6 at a ratio of 3:1. The cells were then homogenized and applied to Ni-NTA columns as described in *SI Appendix*. Control unmixed cells were treated similarly except that buffer was added to give the same volume. Bound proteins were eluted and analyzed on immunoblots using anti-His or M2 anti-FLAG antibodies. (*B*) Chromosomally encoded MgtS-GG-FLAG and MgtA-HA copurify. Cells expressing MgtS-GG-FLAG or MgtS-D30A-GG-FLAG with or without MgtA-HA (GSO777, GSO779, GSO778, and GSO780), all from the chromosome, grown for 2.5 h in N medium without added Mg^{2+}, were homogenized and applied to Pierce anti-HA agarose as described in *SI Appendix*. Aliquots of cells (c) taken before lysis and bound proteins eluted from the beads (b) were analyzed on immunoblots using anti-His or M2 anti-FLAG antibodies.

for MgtS-D30A-GG-FLAG mixed with MgtA-His_6, indicating decreased binding of the partially active D30A mutant.

In a second experiment, exponentially growing cells with a chromosomally encoded MgtS-GG-FLAG or MgtS-D30A-GG-FLAG fusion with and without chromosomally encoded MgtA-HA were placed in N medium without added Mg^{2+} for 2 h to induce the expression of the fusion proteins from their native promoters. Cells were homogenized and incubated with DDM as above and then applied to anti-HA agarose beads. After washing, the proteins retained on the beads were eluted and examined by immunoblot analysis with anti-HA and anti-FLAG antibodies (Fig. 3*B*). As expected, MgtA-HA was detected in the eluates for all cells carrying the gene for this fusion. The FLAG-tagged MgtS derivatives were not detected in the eluates from cells without MgtA-HA. Although the level of the MgtS-GG-FLAG protein was lower than the level of the MgtS-D30A-GG-FLAG protein in the extracts of the cells coexpressing MgtA-HA, the wild-type protein was strongly enriched by copurification with MgtA-HA (30-fold) in contrast to the mutant protein (0.7-fold). These results with endogenous protein levels further support the conclusion that MgtS associates with MgtA.

Effect of MgtS Is Reduced in an *mgtA* Deletion Background. To understand the biological consequences of the MgtS–MgtA interaction, we examined the effects of MgtS on growth and 5′-UTR_{mgtA}-*lacZ* reporter activity in a Δ*mgtA* background. In the Δ*mgtS* strain, complementation with the empty pBAD24 vector resulted in a reduced final OD_{600}, whereas complementation with wild-type *mgtS* increased the final OD_{600} in limited Mg^{2+} (7.5 μM) (Fig. 4*A*). The Δ*mgtA* Δ*mgtS* double mutant with pBAD24 empty vector reached a lower OD_{600} than the Δ*mgtS* mutant alone and MgtS overexpression did not rescue this double mutant phenotype, suggesting that MgtS is acting through MgtA. We observed similar results with the P_{lac}-5′-UTR_{mgtA}-*lacZ* reporter assay. For the vector control strains, the 5′-UTR_{mgtA}-*lacZ* fusion was induced 2.5-fold in the Δ*mgtS* mutant and 3.7-fold in the Δ*mgtA* Δ*mgtS* mutant. With MgtS overproduction, the induction in the Δ*mgtS* background decreased to 0.8-fold, whereas induction was 3.4-fold in the Δ*mgtA* Δ*mgtS* double mutant. Together these results show that effects of MgtS are lost in the Δ*mgtA* background consistent with MgtS acting through MgtA at limiting Mg^{2+} concentrations.

MgtS Modulates MgtA Protein Levels. MgtS could be influencing the levels or the activity of the Mg^{2+} transporter. Thus, we examined the effect of MgtS on MgtA levels by monitoring chromosomally encoded MgtA-HA at different time points after a shift to N medium without added Mg^{2+} in either the wild-type or Δ*mgtS* backgrounds (Fig. 5*A*). Wild-type cells consistently had higher MgtA-HA levels upon Mg^{2+} limitation compared with Δ*mgtS* cells, suggesting that MgtS is important for establishing high MgtA levels. This conclusion was supported by the observation that there were high MgtA levels in strains overexpressing MgtS compared with the vector control strain (Fig. 5*B*). We also compared the levels of MgtA-HA in cells exposed to a 30-min pulse or continuous MgtS expression. There was no decrease from the initial MgtA-HA levels after 30 min of MgtS synthesis, but sustained MgtS expression resulted in significantly higher MgtA-HA levels (Fig. 5*C*), suggesting that MgtA accumulation requires continued MgtS production.

Given that FtsH weakly copurifies with wild-type tagged MgtS, we wondered whether MgtS might be acting to block MgtA cleavage by the FtsH protease. However, directly assaying the effect of loss of *ftsH* on MgtA levels proved difficult, as the *ftsH* mutant strains were unable to grow in the Mg^{2+}-limited N media in which we observed MgtA expression. To circumvent this problem, we overexpressed the bacteriophage λ-cII protein, a known substrate of FtsH (23), as a competitor. In contrast to the vector control strain, MgtA was observed to accumulate in the Δ*mgtS* strain overexpressing cII (Fig. 5*D*).

Overall, these results indicate that MgtS stabilizes MgtA by inhibiting FtsH, leading to increased levels of MgtA in the inner membrane and presumably higher Mg^{2+} import and thus higher intracellular Mg^{2+} when the cation is most limiting. Consistent with this interpretation, we found that overexpression of MgtA was able to partially suppress the Δ*mgtS* effect on P_{lac}-5′-UTR_{mgtA}-*lacZ* induction (*SI Appendix*, Fig. S3).

Discussion

Increasing numbers of small membrane proteins are being identified in a range of organisms, but their functions are largely unknown. In this study, we found that the 31-amino acid PhoPQ-regulated MgtS protein modulates intracellular Mg^{2+} levels to

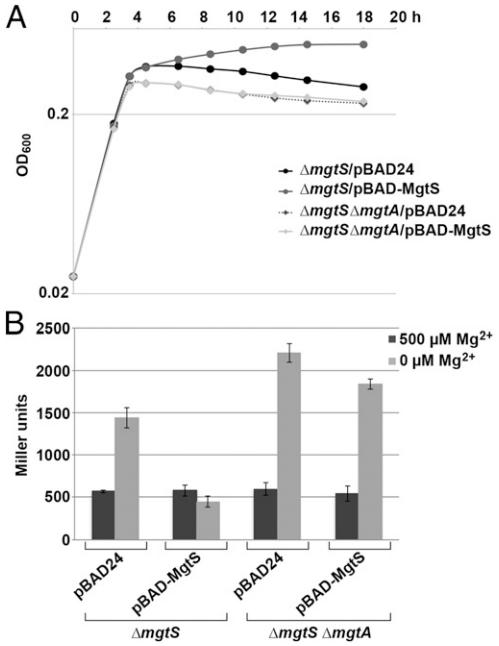

Fig. 4. MgtS acts via MgtA. (*A*) The ability of MgtS overexpression to complement the Δ*mgtS* growth curve defect requires *mgtA*. The OD_{600} of cultures of Δ*mgtS* (GSO775) and Δ*mgtS* Δ*mgtA* (GSO781) carrying pBAD24 or pBAD-MgtS were measured at the indicated times as in Fig. 1*C*. The average of three cultures is shown. (*B*) Repression of Mg^{2+}-reporter activity by MgtS is dependent on *mgtA*. β-Galactosidase activity was assayed for cultures of P_{lac}-*mgtA* 5′-UTR-*lacZ* Δ*mgtS* (GSO774) or P_{lac}-*mgtA* 5′-UTR-*lacZ* Δ*mgtS* Δ*mgtA* (GSO782) cells carrying pBAD24 or pBAD24-MgtS cells as described in *SI Appendix*. The average of three independent trials is shown, and the error bars represent one SD.

maintain cellular integrity upon Mg^{2+} limitation. We report that MgtS is synthesized under conditions of extreme Mg^{2+} limitation, associates with the Mg^{2+} transporter MgtA, and increases the levels of MgtA. A critical tool in our characterization of MgtS was the development of a functional tagged derivative. One barrier in the study of small proteins has been the fact that even the shortest affinity tags contribute substantially to the size of a small protein and some tags are even longer than the protein itself and thus have a greater potential for impacting activity, stability or localization than for a higher molecular weight protein.

The effect of MgtS on MgtA adds to the extensive regulation that has already been described for this high-affinity Mg^{2+} transporter in *S. enterica* and *E. coli*. First, transcription initiation of the *mgtA* locus is controlled by the PhoP two-component response regulator (24). Second, the *mgtA* mRNA has a long 5′-UTR, used as a tool in this study, which encodes an Mg^{2+}-responsive riboswitch (19) as well as a proline-rich leader peptide that renders transcription elongation and translation responsive to proline and Mg^{2+} levels (21, 25). In *S. enterica*, the small MgtR protein reduces MgtA stability (14). Additionally, the activity of the transporter in vitro was recently found to be elevated by cardiolipin and inhibited by high concentrations of Mg^{2+} (22). We now show that the PhoPQ-dependent small MgtS protein appears to enhance MgtA stability in low Mg^{2+} in *E. coli*. Interestingly, MgtS levels reciprocally were lower in a Δ*mgtA* background, suggesting the MgtA also stabilizes MgtS (*SI Appendix*, Fig. S4).

The observations above evoke the question of why synthesis of this Mg^{2+} transporter is so extensively regulated. Several possibilities can be considered. First, MgtA has been shown to transport cations other than Mg^{2+} (26), and tight repression of MgtA levels and activity under all conditions other than Mg^{2+} limitation might be needed to protect against osmotic stress. Second, tight regulation at each step of MgtA synthesis allows for a graded response to different Mg^{2+} concentrations. Third, a number of feedback loops, which control the timing and extent of PhoPQ activation, have been described (27). PhoPQ activation of MgtS, which in turn increases intracellular Mg^{2+} levels, represents yet another such loop.

It is noteworthy that several other small proteins modulate target protein stability both positively and negatively. The aforementioned MgtR decreases the stability of both MgtC and MgtA in *S. enterica* by promoting an interaction with the FtsH protease (14). In contrast, the 26-aa SpoVM protein of *Bacillus subtilis* (28) and the 44-aa cIII protein of bacteriophage λ (29) competitively inhibit FtsH and thus can stabilize substrate proteins. Given that FtsH weakly copurifies with wild-type tagged MgtS, we suggest that MgtS is similarly acting to block FtsH. The finding that the C-terminal D30 and D31 amino acids are essential for MgtS activity is noteworthy in the context of reports that aspartic acid

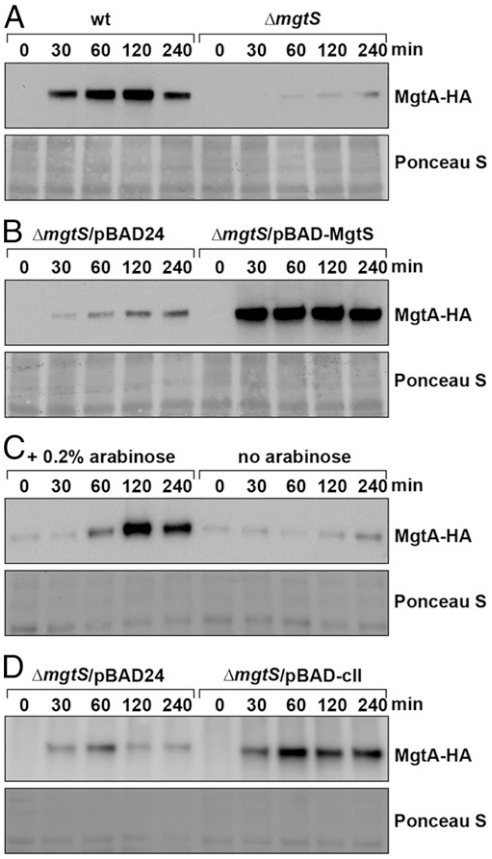

Fig. 5. MgtS modulates MgtA stability. (*A*) Chromosomally encoded MgtA levels are lower in a Δ*mgtS* strain upon Mg^{2+} depletion. Cultures of *mgtS*$^{+}$ *mgtA-HA* (GSO784) and Δ*mgtS mgtA-HA* (GSO786) were grown in N medium with 1 mM Mg^{2+} to OD_{600} ~0.4–0.6, whereupon one aliquot was taken (0 min). The remaining cells were washed and incubated with N medium without added Mg^{2+} as described in *SI Appendix*. (*B*) Chromosomally encoded MgtA levels are elevated upon MgtS overexpression. Cultures of Δ*mgtS mgtA-HA* (GSO786) cells carrying pBAD24 or pBAD24-MgtS were treated as in *A*, except that after cells were washed, arabinose was added. (*C*) MgtA accumulation requires continued MgtS production. Cultures of Δ*mgtS mgtA-HA* (GSO786) cells carrying pBAD24-MgtS were grown as in *B*, except that after 30 min in N medium with arabinose but lacking Mg^{2+}, one aliquot was taken (0 min), and the remaining culture was split and one fraction was washed and grown in N medium lacking Mg^{2+} and arabinose, whereas the second fraction was washed and grown in N medium lacking Mg^{2+} with arabinose. (*D*) MgtA is stabilized by overexpression of the FtsH substrate cII. Overnight cultures of Δ*mgtS mgtA-HA* (GSO786) cells carrying pBAD24 or pBAD24-cII were treated as in *B*. In *A*–*D*, aliquots taken at each time point indicated were pelleted, resuspended to OD_{600} ~50 in SDS loading buffer, and separated by SDS/PAGE for immunoblot analysis using anti-HA antibodies.

MICROBIOLOGY

residues block FtsH-mediated degradation (30, 31). We were unable to directly test the effects of the membrane protease on MgtA levels because *ftsH* is essential and, even with suppressor mutations, strains lacking *ftsH* did not grow in N medium with limited Mg^{2+}. However, overexpression of cII as an FtsH substrate competitor increased MgtA levels in the Δ*mgtS* background, strongly suggesting that MgtA is indeed an FtsH substrate.

MgtS also fits the reoccurring theme that small proteins modulate transporters. Previous studies showed that the 49-aa *E. coli* AcrZ protein affects the specificity of the AcrAB-TolC efflux pump (32) by binding to a specific transmembrane groove in the inner membrane component AcrB (33). The 42-aa *E. coli* MntS protein is proposed to inhibit the MntP transporter, thus blocking Mn^{2+} export when intracellular Mn^{2+} levels are low, though an interaction between the two proteins has not been demonstrated (34). A final example is the mammalian sarcoplasmic reticulum Ca^{2+}-ATPase (SERCA) membrane pump responsible for the reuptake of Ca^{2+} during muscle relaxation, which has been found to be inhibited by three small transmembrane-domain proteins, 31-aa sarcolipin (SLN), 52-aa phospholamban (PLN), 46-aa myoregulin (MLN) (35), and activated by a fourth, 34-aa DWORF (36). Intriguingly, both the MgtA and SERCA cation pumps are P-type ATPases, and MgtA has been reported to share biochemical properties with SERCA (22). It will be interesting to see how many other P-type ATPases are modulated by small proteins and whether features of the small proteins can be exploited to activate, modify, or block these important transporters.

Materials and Methods

Strains and Plasmids. All strains are derivatives of a laboratory stock of *E. coli* K-12 MG1655 unless noted otherwise and are listed in Dataset S1. Plasmids used in this study are listed in Dataset S1. Details about strain and plasmid construction are provided in *SI Appendix*. The oligonucleotides used in these constructions are listed in Dataset S1.

Bacterial Growth. Cells were cultured in Luria broth (LB) or N-minimal medium (pH 7.4) (37) (N medium) at 37 °C with indicated concentrations of Mg^{2+} as described in *SI Appendix*.

Northern and Immunoblot Analysis. Specific RNAs were detected by Northern analysis with oligonucleotide probes and tagged proteins as well as GroEL were detected by immunoblot analysis using commercially available antibodies as described in detail in *SI Appendix*.

β-Galactosidase Assays. β-Galactosidase activity was assayed as described (38); specific details are provided in *SI Appendix*.

Tagged Protein Purification. The FLAG-, His_6- and HA-tagged proteins were purified based on their tags using commercial resins as described in detail in *SI Appendix*.

ACKNOWLEDGMENTS. We thank P. Backlund for conducting mass spectrometric analysis; S. Adhya and F. Narberhaus for reagents; E. Groisman, M. Machner, and K. Ramamurthi for helpful experimental suggestions; and K. Ramamurthi and J. Vogel for comments on the manuscript. Work in the G.S. laboratory is supported by the Intramural Program of the Eunice Kennedy Shriver National Institute of Child Health and Human Development.

1. Salazar ME, Laub MT (2015) Temporal and evolutionary dynamics of two-component signaling pathways. *Curr Opin Microbiol* 24:7–14.
2. Groisman EA, et al. (2013) Bacterial Mg^{2+} homeostasis, transport, and virulence. *Annu Rev Genet* 47:625–646.
3. Prost LR, Miller SI (2008) The Salmonellae PhoQ sensor: Mechanisms of detection of phagosome signals. *Cell Microbiol* 10:576–582.
4. Dalebroux ZD, Miller SI (2014) Salmonellae PhoPQ regulation of the outer membrane to resist innate immunity. *Curr Opin Microbiol* 17:106–113.
5. Storz G, Wolf YI, Ramamurthi KS (2014) Small proteins can no longer be ignored. *Annu Rev Biochem* 83:753–777.
6. Hemm MR, Paul BJ, Schneider TD, Storz G, Rudd KE (2008) Small membrane proteins found by comparative genomics and ribosome binding site models. *Mol Microbiol* 70:1487–1501.
7. Hemm MR, et al. (2010) Small stress response proteins in *Escherichia coli*: Proteins missed by classical proteomic studies. *J Bacteriol* 192:46–58.
8. Lippa AM, Goulian M (2009) Feedback inhibition in the PhoQ/PhoP signaling system by a membrane peptide. *PLoS Genet* 5:e1000788.
9. Salazar ME, Podgornaia AI, Laub MT (2016) The small membrane protein MgrB regulates PhoQ bifunctionality to control PhoP target gene expression dynamics. *Mol Microbiol* 102:430–445.
10. Lippa AM, Goulian M (2012) Perturbation of the oxidizing environment of the periplasm stimulates the PhoQ/PhoP system in *Escherichia coli*. *J Bacteriol* 194:1457–1463.
11. Cardenal-Muñoz E, Ramos-Morales F (2013) DsbA and MgrB regulate *steA* expression through the two-component system PhoQ/PhoP in *Salmonella enterica*. *J Bacteriol* 195:2368–2378.
12. Alix E, Blanc-Potard AB (2008) Peptide-assisted degradation of the *Salmonella* MgtC virulence factor. *EMBO J* 27:546–557.
13. Lee EJ, Pontes MH, Groisman EA (2013) A bacterial virulence protein promotes pathogenicity by inhibiting the bacterium's own F_1F_o ATP synthase. *Cell* 154:146–156.
14. Choi E, Lee KY, Shin D (2012) The MgtR regulatory peptide negatively controls expression of the MgtA Mg^{2+} transporter in *Salmonella enterica* serovar Typhimurium. *Biochem Biophys Res Commun* 417:318–323.
15. Wassarman KM, Repoila F, Rosenow C, Storz G, Gottesman S (2001) Identification of novel small RNAs using comparative genomics and microarrays. *Genes Dev* 15:1637–1651.
16. Fontaine F, Fuchs RT, Storz G (2011) Membrane localization of small proteins in *Escherichia coli*. *J Biol Chem* 286:32464–32474.
17. Moon K, Gottesman S (2009) A PhoQ/P-regulated small RNA regulates sensitivity of *Escherichia coli* to antimicrobial peptides. *Mol Microbiol* 74:1314–1330.
18. Zeghouf M, et al. (2004) Sequential Peptide Affinity (SPA) system for the identification of mammalian and bacterial protein complexes. *J Proteome Res* 3:463–468.
19. Cromie MJ, Shi Y, Latifi T, Groisman EA (2006) An RNA sensor for intracellular $Mg^{(2+)}$. *Cell* 125:71–84.
20. Korth MM, Sigel RK (2012) Unusually high-affinity $Mg^{(2+)}$ binding at the AU-rich sequence within the antiterminator hairpin of a $Mg^{(2+)}$ riboswitch. *Chem Biodivers* 9:2035–2049.
21. Gall AR, et al. (2016) Mg^{2+} regulates transcription of *mgtA* in *Salmonella* Typhimurium via translation of proline codons during synthesis of the MgtL peptide. *Proc Natl Acad Sci USA* 113:15096–15101.
22. Subramani S, Perdreau-Dahl H, Morth JP (2016) The magnesium transporter A is activated by cardiolipin and is highly sensitive to free magnesium in vitro. *eLife* 5:e11407.
23. Shotland Y, et al. (1997) Proteolysis of the phage lambda CII regulatory protein by FtsH (HflB) of Escherichia coli. *Mol Microbiol* 24:1303–1310.
24. Minagawa S, et al. (2003) Identification and molecular characterization of the Mg^{2+} stimulon of *Escherichia coli*. *J Bacteriol* 185:3696–3702.
25. Park SY, Cromie MJ, Lee EJ, Groisman EA (2010) A bacterial mRNA leader that employs different mechanisms to sense disparate intracellular signals. *Cell* 142:737–748.
26. Snavely MD, Florer JB, Miller CG, Maguire ME (1989) Magnesium transport in *Salmonella typhimurium*: $^{28}Mg^{2+}$ transport by the CorA, MgtA, and MgtB systems. *J Bacteriol* 171:4761–4766.
27. Park SY, Groisman EA (2014) Signal-specific temporal response by the *Salmonella* PhoP/PhoQ regulatory system. *Mol Microbiol* 91:135–144.
28. Cutting S, et al. (1997) SpoVM, a small protein essential to development in Bacillus subtilis, interacts with the ATP-dependent protease FtsH. *J Bacteriol* 179:5534–5542.
29. Halder S, Banerjee S, Parrack P (2008) Direct CIII-HflB interaction is responsible for the inhibition of the HflB (FtsH)-mediated proteolysis of Escherichia coli sigma(32) by lambdaCIII. *FEBS J* 275:4767–4772.
30. Führer F, Langklotz S, Narberhaus F (2006) The C-terminal end of LpxC is required for degradation by the FtsH protease. *Mol Microbiol* 59:1025–1036.
31. Kobiler O, Koby S, Teff D, Court D, Oppenheim AB (2002) The phage lambda CII transcriptional activator carries a C-terminal domain signaling for rapid proteolysis. *Proc Natl Acad Sci USA* 99:14964–14969.
32. Hobbs EC, Yin X, Paul BJ, Astarita JL, Storz G (2012) Conserved small protein associates with the multidrug efflux pump AcrB and differentially affects antibiotic resistance. *Proc Natl Acad Sci USA* 109:16696–16701.
33. Du D, et al. (2014) Structure of the AcrAB-TolC multidrug efflux pump. *Nature* 509:512–515.
34. Martin JE, Waters LS, Storz G, Imlay JA (2015) The *Escherichia coli* small protein MntS and exporter MntP optimize the intracellular concentration of manganese. *PLoS Genet* 11:e1004977.
35. Anderson DM, et al. (2015) A micropeptide encoded by a putative long noncoding RNA regulates muscle performance. *Cell* 160:595–606.
36. Nelson BR, et al. (2016) A peptide encoded by a transcript annotated as long noncoding RNA enhances SERCA activity in muscle. *Science* 351:271–275.
37. Hmiel SP, Snavely MD, Miller CG, Maguire ME (1986) Magnesium transport in *Salmonella typhimurium*: Characterization of magnesium influx and cloning of a transport gene. *J Bacteriol* 168:1444–1450.
38. Miller JH (1992) *A Short Course in Bacterial Genetics: A Laboratory Manual and Handbook for Escherichia coli and Related Bacteria* (Cold Spring Harbor Lab Press, Plainview, NY).